Unified transverse diffeomorphism invariant field theory for the dark sector

David Alonso-López[*]

Departamento de Física de la Tierra y Astrofísica, Universidad Complutense de Madrid,
28040 Madrid, Spain

Javier de Cruz Pérez[†] and Antonio L. Maroto[‡]

Departamento de Física Teórica and Instituto de Física de Partículas y del Cosmos (IPARCOS-UCM),
Universidad Complutense de Madrid, 28040 Madrid, Spain

In this work we present a unified model for the cosmological dark sector. The theory is based on a simple minimally coupled scalar field whose action only contains a canonical kinetic term and is invariant under transverse diffeomorphisms (TDiff). The model has the same number of free parameters as lambda cold dark matter (ΛCDM). We confront the predictions of the model at the background level with data from Planck 2018 CMB distance priors, Pantheon+ and SH0ES SNIa distance moduli, BAO data points from 6dFGS, BOSS, eBOSS and DES and measurements of the Hubble parameter from cosmic chronometers. The model provides excellent results in the joint fit analysis, showing strong and very strong evidence compared to ΛCDM in the Bayesian evidence and deviance information criterion (DIC) respectively. We also show that the Hubble tension between Planck 2018 and SH0ES measurements can be alleviated in the unified TDiff model although further analysis is still needed.

I. INTRODUCTION

General relativity's (GR) symmetry group is the group of diffeomorphisms (Diff). This symmetry arises as a consequence of Einstein's equivalence principle (EEP) which states geodesic motion, Lorentz invariance and local position invariance (LPI) [1,2]; which in turn translates into the principle of general covariance. This principle essentially means that a physical equation is generally covariant, i.e., it remains in the same form under a general coordinate transformation [2]. When performing an infinitesimal diffeomorphism generated by the vector field $\xi^\mu(x)$

$$\hat{x}^\mu = x^\mu + \xi^\mu(x), \tag{1}$$

the metric tensor transforms with the Lie derivative, i.e., $\delta g_{\mu\nu} = \mathcal{L}_\xi g_{\mu\nu} = -2\nabla_{(\mu}\xi_{\nu)}$. Consider now the action

$$S = S_{\mathrm{EH}}[g_{\mu\nu}] + S_m[g_{\mu\nu}, \psi^i], \tag{2}$$

where

$$S_{\mathrm{EH}} = -\frac{1}{16\pi G} \int d^4x \sqrt{g} R, \tag{3}$$

is the Einstein-Hilbert action, $g \equiv |\det(g_{\mu\nu})|$ and $S_m[g_{\mu\nu}, \psi^i]$ is the matter action that depends on the metric tensor as well as on the matter fields ψ^i. Diffeomorphism invariance implies $\delta_\xi S = 0$, which, in turn, implies the conservation of the energy-momentum tensor over solutions of the equations of motion of the matter fields [3],

$$\nabla_\mu T^{\mu\nu} = 0. \tag{4}$$

The purpose of this work is to study the breaking of this symmetry down to transverse diffeomorphisms (TDiff) in the matter sector. In 1919 Einstein himself was the first to introduce unimodular gravity [4], where the determinant of the metric tensor is subject to the condition $g = 1$. As a result, the dynamical equations are the traceless Einstein's equations and the symmetry group is TDiff, i.e. diffeomorphisms subject to the condition

$$\partial_\mu \xi^\mu = 0. \tag{5}$$

The main appeal of this theory is that a cosmological constant-type term does not gravitate which could provide a solution to the vacuum-energy problem [5]. Note that in these theories the symmetry is broken in the geometrical sector, however more recently the effects of Diff breaking in the matter sector have been explored in [6–8] for simple scalar field theories. There, it is shown that these models behave as ordinary Diff invariant theories in the geometric

[*]dalons07@ucm.es
[†]jadecruz@ucm.es
[‡]maroto@ucm.es

optics approximation, i.e., for modes well inside the Hubble radius, where we recover the standard propagation properties of free particles along geodesics, together with the standard scaling of energy density for relativistic and nonrelativistic particles. However for long-wavelength modes, with frequencies smaller than the Hubble parameter, the behavior can be drastically different from that of the Diff models, thus opening a new avenue for cosmological model building.

Particularly simple cases are the minimally coupled TDiff scalar theories with purely kinetic terms. These models are modifications of the Diff scalar theories parametrized by a single function of the metric determinant $f(g)$. They have been seen to be equivalent to perfect adiabatic fluids with an effective equation of state given by [7,8]

$$\omega_\phi = \frac{F}{1-F},\qquad(6)$$

with

$$F = \frac{d\ln f}{d\ln g},\qquad(7)$$

In particular, for simple power law models $f(g) = g^\alpha$, the equation of state is just a constant given by

$$\omega_\phi = \frac{\alpha}{1-\alpha},\qquad(8)$$

which as expected, recovers the standard stiff fluid behavior $\omega_\phi = 1$ in the Diff case with $\alpha = 1/2$. However, other choices are possible. Thus models with $\alpha = 0$ would behave as nonrelativistic matter fluid, not only at the background level but also for perturbations, since in this simple case $c_s^2 = \omega_\phi = 0$ (being c_s the speed of sound) providing an extremely simple model for dark matter based on a purely kinetic scalar field.

The simplicity of these results suggests the possibility of using these kinetic TDiff models for a unified description of the dark sector with a single field. With that purpose, appropriate $f(g)$ functions which allow an interpolation between a dark matter behavior at early times and a dark energy behavior at late times should be identified.

The first unification models considered in the literature were based on the so called generalized Chaplygin gas [9]. These models are based on a single perfect fluid description of the dark sector with an equation of state given by

$$p = -A\frac{1}{\rho^\alpha},\qquad(9)$$

with A a positive constant so that for $\alpha > 0$ the behavior is the expected for the dark sector. As a matter of fact, at the background level, the cosmological evolution in this model allows to reduce the H_0 tension to the 1σ level [10].

The model contains one extra parameter compared to ΛCDM. When comparing the matter power spectrum with LSS data a stringent limit on the extra parameter is introduced, so that $|\alpha| \lesssim 10^{-5}$, [11]. This constraint implies that the model effectively behaves as ΛCDM and the solution of the tension is no longer achieved. Imperfect fluid models with bulk viscosity have also been considered for an unified description in [12].

Unified models built out of a single scalar field have also been proposed in recent years. Thus, certain k-essence models with a Lagrangian density

$$\mathcal{L} = G(X),\qquad(10)$$

with $X = \frac{1}{2}g^{\mu\nu}\partial_\mu\phi\partial_\nu\phi$ and $G(X)$ a quadratic function of X have been proposed in [13]. The model avoids the problem with the matter power spectrum measurements, although the price to pay in this case is the inclusion of four extra parameters as compared to ΛCDM.

In this work we will start the analysis of the possibilities of purely kinetic TDiff theories for the construction of viable unification models. We will limit ourselves to the background evolution and the comparison with observables related to the expansion history, in particular Hubble diagrams from SNIa Pantheon+&SH0ES, cosmic chronometers, BAO measurements and CMB distance priors.

This paper is organized as follows: in Sec. II we present some general aspects of TDiff invariant actions for scalar fields, we derive the equations of motion for the field and the consistency condition that ensures conservation of the energy-momentum tensor for TDiff theories. In Sec. III we build the unified model for the dark sector, where we find Einstein's equations for our universe, which take the simple usual form of the Friedmann and acceleration equations. We give the expression for the energy density of the scalar field, treated as a perfect fluid and present the Hubble rates of the theory. In Sec. IV we present the cosmological data we used to build the likelihood to find the constraints on the parameters of the model. Section V is devoted to present and discuss the results of the fitting process and in Sec. VI we present our conclusions. Finally, in the Appendix we show the basic derivation of the TDiff invariant action for a scalar field.

Throughout this manuscript we will use the metric signature $(+,-,-,-)$ and natural units $\hbar = c = 1$.[1]

II. TDiff INVARIANT ACTION FOR A SCALAR FIELD

Let us start by writing the TDiff invariant action for a simple minimally coupled scalar field in the kinetic regime (see the Appendix for details)

---

[1]The Hubble parameter H_0 will be expressed sometimes in units of km/s/Mpc to ease the comparison with other results in the literature where this convention is commonly used.

$$S = S_{\text{EH}} + S_\phi$$
$$= -\frac{1}{16\pi G} \int d^4x \sqrt{g} R + \int d^4x f(g) \frac{1}{2} g^{\mu\nu} \partial_\mu \phi \partial_\nu \phi, \quad (11)$$

where $f(g)$ is a positive function of the metric determinant. This guarantees a stable theory which respects the weak equivalence principle in the geometric optics approximation [7]. The gravitational sector is described by the standard Einstein-Hilbert action so that only the scalar sector breaks Diff invariance down to TDiff.[2] Notice that the standard Diff invariant theory is recovered in the case $f(g) = \sqrt{g}$.

A. TDiff models in cosmological backgrounds

We now would like to specify the geometry in order to build cosmological models for homogeneous scalar fields, i.e. coupled to a homogeneous and isotropic spacetime such as Robertson-Walker (RW). In this cosmological case, in which we have a spacetime whose constant time hypersurfaces are maximally symmetric subspaces, symmetry implies that, in the general case, only 2 metric components are truly independent, up to the sign of the curvature of these hypersurfaces. We will work with flat spatial sections, so the line element of the most general homogeneous and isotropic spacetime is [2]

$$ds^2 = b^2(\tau) d\tau^2 - a^2(\tau) d\vec{x}^2, \quad (12)$$

where $a(\tau)$ and $b(\tau)$ are the two independent components of the metric.

It is most common to define a new time coordinate, known as cosmological time $dt = b(\tau) d\tau$ which finally leaves us with only one function $a(t)$ to solve for. Note that this is only possible in the case of a full Diff theory. In general there is no way to perform a coordinate transformation satisfying the TDiff condition that allows us to write (12) using cosmological time $t(\tau)$.

B. Equations of motion for $\phi(\tau)$

The scalar field equations of motion obtained from (11) read

$$\partial_\nu(f(g) g^{\mu\nu} \partial_\mu \phi) = 0. \quad (13)$$

Let us consider the evolution of a homogeneous scalar field only depending on time, so that the equations of motion satisfied by $\phi(\tau)$ in the geometry (12) are [7]

$$\phi'' + \left(\frac{f'}{f} - 2\frac{b'}{b}\right)\phi' = \phi'' + \frac{L'}{L}\phi' = 0, \quad (14)$$

where the prime denotes the derivative with respect to the coordinate time τ, and

$$L(\tau) = \frac{f(g(\tau))}{b^2(\tau)}. \quad (15)$$

It is easy to check that in the $f(g) = \sqrt{g}$ case, we recover the well-known results for a Diff invariant scalar field. Equation (14) can be rewritten as a total derivative

$$\frac{d}{d\tau}(L\phi') = 0, \quad (16)$$

so one immediately obtains [7]

$$\phi'(\tau) = \frac{C_\phi}{L(\tau)}. \quad (17)$$

with C_ϕ a constant.

Even though it is not possible to set $b = 1$ with a TDiff coordinate transformation, we can always rewrite (14) in cosmological time $dt = b(\tau) d\tau$ so that we obtain

$$\ddot{\phi} + \frac{\dot{J}}{J}\dot{\phi} = 0, \quad (18)$$

where

$$J = Lb = \frac{f}{b} = a^3 \frac{f}{\sqrt{g}} \quad (19)$$

and dot denotes derivative with respect to the cosmological time t.

C. Einstein's equations and the energy-momentum tensor

The field equations derived from the action (11) with unconstrained variations with respect to the metric tensor

$$-\frac{2}{\sqrt{g}}\frac{\delta S}{\delta g_{\mu\nu}} = 0, \quad (20)$$

are the Einstein's equations

$$G_{\mu\nu} = 8\pi G T^\phi_{\mu\nu}, \quad (21)$$

where

$$T^\phi_{\mu\nu} = \frac{f(g)}{\sqrt{g}}(\partial_\mu \phi \partial_\nu \phi - F(g) g_{\mu\nu} g^{\alpha\beta} \partial_\alpha \phi \partial_\beta \phi). \quad (22)$$

with $F(g)$ given in (7).

Notice that because of the breaking of Diff invariance in the scalar sector, $T^\phi_{\mu\nu}$ is not necessarily conserved on solutions of the scalar field equations of motion. In spite of that, since Einstein's equations (21) still hold, Bianchi identities imply the conservation of the energy-momentum tensor (22) over solutions of the Einstein's equations.

---

[2]See [14] for a detailed study of gravity models which break Diff invariance in the geometrical part of the action.

Since our goal is to build a cosmological model, we would like to interpret our field as a perfect fluid,[3] whose energy-momentum tensor is well-known to be parametrized as

$$T^{\mu\nu}_\phi = \rho_\phi u^\mu u^\nu - p_\phi h^{\mu\nu}, \qquad (23)$$

where u^μ is the 4-velocity of the fluid, and as such it must obey the normalization condition $g_{\mu\nu} u^\mu u^\nu = 1$, and $h_{\mu\nu} = g_{\mu\nu} - u_\mu u_\nu$ is the metric tensor on the hypersurfaces orthogonal to the direction of the timelike vector u^μ. We can read the energy density ρ_ϕ and the pressure p_ϕ of our fluid to be

$$\rho_\phi = T^{00}_\phi g_{00} = \frac{f(g)}{b^2 \sqrt{g}} (1 - F(g)) \phi'^2, \qquad (24)$$

$$p_\phi = -\frac{T^i_{\phi i}}{3} = \frac{f(g)}{b^2 \sqrt{g}} F(g) \phi'^2. \qquad (25)$$

From these two expressions we are able to define an equation of state for the fluid in the usual way $p_\phi(a) = \omega_\phi \rho_\phi(a)$, where

$$\omega_\phi = \frac{F}{1 - F}. \qquad (26)$$

Notice that the equation of state parameter solely depends on our choice of $f(g)$. It is worth mentioning that the problematic case $F = 1$ is excluded since it implies $\rho_\phi = 0$ in (24). It is already possible to draw some conclusions on how the fluid behaves from (26). If we had a power law $f \propto g^\alpha$, then

$$\omega_\phi = \frac{\alpha}{1 - \alpha}, \qquad (27)$$

which is time independent. In order to have positive energy density we must have $\alpha < 1$. To recover a nonrelativistic/dark matter type behavior we simply need $\alpha = 0$, whereas $\alpha \to \infty$ implies a cosmological constant behavior $\omega_\phi = -1$. We can interpolate between these two limiting cases with an exponential function $f(g) \propto e^{-\beta g}$, resulting in

$$\omega_\phi = -\frac{\beta g}{1 + \beta g}, \qquad (28)$$

where $\beta g \ll 1 \Rightarrow \omega_\phi = 0$ while $\beta g \gg 1 \Rightarrow \omega_\phi = -1$. The condition required for a positive energy density is now $\beta g > -1$ [7].

Computing $\nabla_\mu T^{\mu\nu}_\phi$ yields[4]

$$\nabla_\mu T^{\mu\nu}_\phi = u^\nu (u^\mu \nabla_\mu \rho_\phi + (\rho_\phi + p_\phi) \nabla_\mu u^\mu)$$
$$= \frac{u^\nu}{b} \left(\rho'_\phi + 3 \frac{a'}{a} (\rho_\phi + p_\phi) \right) = 0. \qquad (29)$$

As expected for a RW geometry, there is actually just one independent equation[5]

$$\rho'_\phi + 3 \frac{a'}{a} (\rho_\phi + p_\phi) = 0. \qquad (30)$$

The compatibility of Eq. (30) and the equations of motion of the field (14) will impose a condition on $b(\tau)$. Though not always possible to find such a condition in an explicit way, in the kinetic domination regime it can actually be realized [7]. By expressing ρ'_ϕ in terms of ρ_ϕ, which requires the use of the equations of motion (14), since $\rho_\phi + p_\phi = \rho_\phi/(1 - F)$ we get rid of the energy density explicit dependence and only terms involving the geometry b, a, and $f(g)$ will appear. After some manipulations we find

$$\frac{g'}{g} \left(F - \frac{1}{2} \right) + \frac{F'}{1 - F} = 6 \left(\frac{a'}{a} \right) \frac{F - \frac{1}{2}}{1 - F}, \qquad (31)$$

which is written in such a way that is trivially satisfied when $F = 1/2 \Rightarrow F' = 0$. Multiplying both sides by $(1 - F)/(F - 1/2)$ we finally arrive at[6]

$$\frac{g'}{g} (1 - F) - \frac{2F'}{1 - 2F} = 6 \frac{a'}{a}. \qquad (32)$$

Integration yields [7]

$$\frac{g}{f(g)} (1 - 2F(g)) = C_g a^6, \qquad (33)$$

with C_g a constant. For TDiff invariant models, we must solve this equation for a given $f(g)$ in order to have a conserved energy-momentum tensor. This will give us a relation between the two functions $b(\tau)$ and $a(\tau)$, i.e., $b(a)$.

---

[3]See [8] for a discussion of the condition to be met in order to describe the scalar field component that breaks Diff invariance down to TDiff as a perfect fluid.

[4]We have used the fact that for a homogeneous and isotropic geometry there are no pressure gradients at a given spacelike hypersurface of $\tau =$ const, i.e., $h^{\mu\nu} \nabla_\mu p = 0$; which ensures geodesic motion $u^\mu \nabla_\mu u^\nu = 0$.

[5]Note that despite the fact that b' does not explicitly appear on (30), the energy density and the pressure of the fluid do depend on $b(\tau)$, and hence a dependence on b' is implicit in ρ'_ϕ.

[6]Note that this expression no longer recovers the GR identity as a consequence of implicitly dividing by zero when $F = 1/2$ in the last step of the derivation.

III. A UNIFIED MODEL FOR THE DARK SECTOR

Once we have discussed what it means to have a TDiff invariant action for a scalar field, and what conditions must be satisfied in order to build a consistent model with it, we shall put this knowledge to use to construct a TDiff invariant theory for the dark sector in cosmology. We would like to extend the action in (11) to also account for the well-known physics, that is, the particles of the Standard Model. To do so, we proceed as usual by including a full Diff action for baryonic matter (B) and photons plus massless neutrinos, which will be referred to as radiation (R), all of them treated as perfect fluids.

So, how to model dark matter and dark energy with a single TDiff invariant scalar field? As discussed in last section, we saw that for an exponential function

$$f(g) = e^{-\beta g} \tag{34}$$

we could interpolate between a matter-type behavior at early times ($\omega_\phi(a \to 0) = 0$) and a cosmological constant-type one ($\omega_\phi(a \to 1) = -1$) at late times. This will be our choice since it allows for a unified description for both dark matter and dark energy. The action reads

$$S = S_{EH} + S_{B+R} + S_\phi, \tag{35}$$

where S_{EH} is given in (3), S_{B+R} takes into account the baryon and radiation contributions, and

$$S_\phi = \int d^4x e^{-\beta g} \left(\frac{1}{2} g^{\mu\nu} \partial_\mu \phi \partial_\nu \phi \right), \tag{36}$$

for the TDiff scalar sector. This means that Einstein's equations are

$$G_{\mu\nu} = 8\pi G (T_{\mu\nu}^{B+R} + T_{\mu\nu}^\phi), \tag{37}$$

where $T_{\mu\nu}^{B+R}$ corresponds to the energy-momentum tensor of baryons and radiation and $T_{\mu\nu}^\phi$ represents the contribution from the dark sector. As a good approximation we can consider that baryons and radiation do not interact at the background level with each other which means that both are self-conserved. In the case of baryons the energy density evolves according to $\rho_B(a) = \rho_B a^{-3}$[7] whereas its equation of state is $\omega_B = 0$. The energy density, as a function of the scale factor, of radiation can be written in terms of photon's energy density [$\rho_\gamma(a)$] as follows

$$\rho_R(a) = \left(1 + \frac{7}{8} N_{eff} \left(\frac{4}{11} \right)^{4/3} \right) \rho_\gamma(a), \tag{38}$$

---

[7]When we do not indicate the explicit dependence in the scale factor or in the redshift, for the energy densities we are referring to the corresponding present value.

where $N_{eff} = 3.046$ is the effective number of neutrino species and $\rho_\gamma(a) = \rho_\gamma a^{-4}$. The equation of state for the radiation fluid is $\omega_R = 1/3$. As for the dark sector we can take advantage of the novel result obtained in [8]. In this reference it is shown that, as long as the derivative of the scalar field $\partial_\mu \phi$ is a timelike vector, from the conservation of the energy-momentum tensor, in the kinetic domain, the energy density associated to the scalar field can be expressed as follows

$$\rho_\phi(a) = \frac{C_\phi}{(\omega_\phi - 1)\sqrt{g}}, \tag{39}$$

where C_ϕ is a constant that needs to be fixed so that the cosmic sum rule is fulfilled.

The two independent components of the Einstein tensor are

$$G_{00} = 3 \left(\frac{a'}{a} \right)^2, \tag{40}$$

$$G_{ii} = -2 \left(\frac{a}{b} \right)^2 \left(\frac{a''}{a} - \frac{a'}{a} \frac{b'}{b} + \frac{1}{2} \left(\frac{a'}{a} \right)^2 \right). \tag{41}$$

Using $T_{00} = b^2[\rho_B(a) + \rho_R(a) + \rho_\phi(a)]$ and $T_{ii} = a^2[p_R(a) + p_\phi(a)]$ we get

$$\left(\frac{a'}{a} \right)^2 = \frac{8\pi G}{3} [\rho_B(a) + \rho_R(a) + \rho_\phi(a)]b^2, \tag{42}$$

$$\frac{a''}{a} - \frac{a'}{a} \frac{b'}{b} + \frac{1}{2} \left(\frac{a'}{a} \right)^2 = -4\pi G [p_R(a) + p_\phi(a)]b^2. \tag{43}$$

As we have mentioned before, if we had set $b = 1$ from the beginning, no simultaneous solutions for the field equations (14) and the conservation of energy (33) could have been found [7]. However, once we have obtained the equations of motion, it is possible to perform a change of variables to cosmological time $dt = b(\tau)d\tau$. After doing so we obtain the equivalent to the usual Friedmann and acceleration equations that take the standard form

$$H^2 = \frac{8\pi G}{3} [\rho_B(a) + \rho_R(a) + \rho_\phi(a)], \tag{44}$$

$$\frac{\ddot{a}}{a} = -\frac{4\pi G}{3} [\rho_B(a) + \rho_R(a) + \rho_\phi(a) + 3p_R(a) + 3p_\phi(a)], \tag{45}$$

where we have used (44) to obtain (45) and $H = \dot{a}/a$ is just the Hubble rate. Notice that although at first glance it might look as if there was no explicit $b(t)$ dependence, the energy density and pressure of the dark sector do depend on it. It is there were the consistency relation $b(a)$ (33) comes into

play. Imposing $f(g) = e^{-\beta g}$ and $F(g) = -\beta g$ it can be written as

$$b^2 e^{\beta a^6 b^2} (1 + 2\beta a^6 b^2) = C_g. \qquad (46)$$

We can fix the value of the constant C_g by evaluating the left hand side at present time, namely $a = b = 1$, which automatically implies that the determinant of the metric is normalized as $g(a = 1) = 1$. We end up with the following expression for the constraint

$$b^2 e^{\beta(a^6 b^2 - 1)} \frac{(1 + 2\beta a^6 b^2)}{1 + 2\beta} = 1. \qquad (47)$$

Thanks to the above expression we will be able to get $b = b(a, \beta)$.

The Hubble rate can be obtained from (44)

$$H(a) = H_0 \sqrt{\Omega_B a^{-3} + \Omega_R a^{-4} + \Omega_\phi(a)}, \qquad (48)$$

where we have considered the definitions $\Omega_i(a) \equiv \frac{\rho_i(a)}{\rho_c},^8$ with $i = B, R, \phi$ and being $\rho_c = 3H_0^2/(8\pi G)$ the value today of the critical energy density.

The cosmic sum rule evaluated at present time reads

$$1 = \Omega_B + \Omega_R + \Omega_\phi. \qquad (49)$$

As stated before C_ϕ in (39) can be fixed with relation (49). By doing so we get

$$\Omega_\phi(a) = \Omega_\phi \left(\frac{\omega_\phi(a = 1) - 1}{\omega_\phi(a) - 1} \right) \frac{1}{\sqrt{g}}. \qquad (50)$$

Once we have (47) and (50) we can study the high redshift limit. From (47) we get the following approximation $b \simeq \sqrt{1 + 2\beta} e^{\frac{\beta}{2}}$ which in turn allows us to find an approximate expression for the energy density of the scalar field valid at short times

$$\Omega_\phi(a) \simeq \Omega_{DM}^{eff} a^{-3}, \qquad (51)$$

where we have used

$$\Omega_{DM}^{eff} \equiv \Omega_\phi e^{-\frac{\beta}{2}} \frac{\sqrt{1 + 2\beta}}{1 + \beta}. \qquad (52)$$

This does not come as a surprise since as we have stated previously when $\beta g \ll 1$ the equation of state tends to the value $\omega_\phi = 0$, therefore it behaves as nonrelativistic matter.

At the background level we can separate the contribution of the scalar field as if it were composed of an effective dark

---

matter contribution, whose expression is determined by Eq. (51) and an effective dark energy component:

$$\rho_\phi(a) = \rho_{DM}^{eff}(a) + \rho_{DE}^{eff}(a) = \rho_c \Omega_{DM}^{eff} a^{-3} + \rho_{DE}^{eff}(a), \qquad (53)$$

$$p_\phi(a) = p_{DM}^{eff}(a) + p_{DE}^{eff}(a) = \omega_{DE}^{eff}(a) \rho_{DE}^{eff}(a). \qquad (54)$$

As stated previously, due to the form of the equation of state parameter (28) the scalar field behaves as nonrelativistic matter at early times and as dark energy at late times. Therefore, considering the above equations we can tell when the effective dark energy component has a quintessencelike behavior and when it has a phantomlike behavior. The expression for the equation of state parameter is the following one

$$\omega_{DE}^{eff}(a) = \omega_\phi(a) \frac{\rho_\phi(a)}{\rho_\phi(a) - \rho_{DM}^{eff}(a)}. \qquad (55)$$

As an example, in Fig. 1 we plot its evolution for the values of the cosmological parameters in Table III. As it can be seen, $\omega_{DE}^{eff}(a) \simeq -2$, at high redshift, something that can be checked from the analytical expression (55). This asymptotic value is determined by the particular form of the $f(g)$ function in (34) regardless the specific value of β. The value of $\omega_{DE}^{eff}(a)$ remains in the phantom region for most of the cosmic history, however, as we get closer to present time its value starts to increase until it crosses the phantom divide. This is the opposite of other unified models such as the generalized Chaplygin gas in which no crossing of the phantom divide line occurs in the effective dark energy equation of state. The crossing of the phantom divide line has been shown in [15] to be a necessary condition to solve the H_0 and σ_8 tensions in models of dark energy.
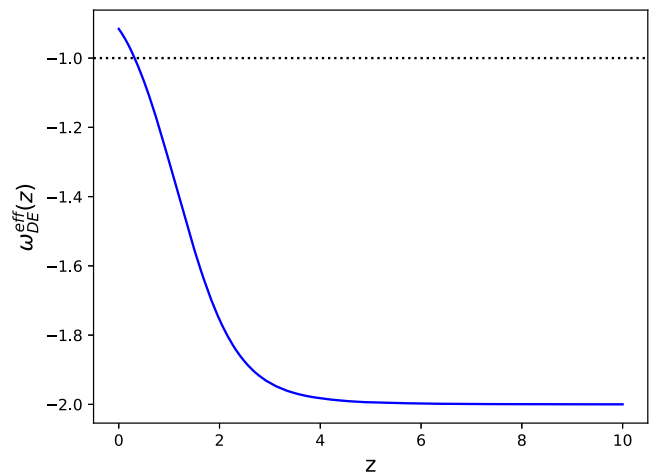

FIG. 1. The effective equation of state parameter of the dark energy component for the TDiff model (55). The values of the cosmological parameters can be seen in Table III.

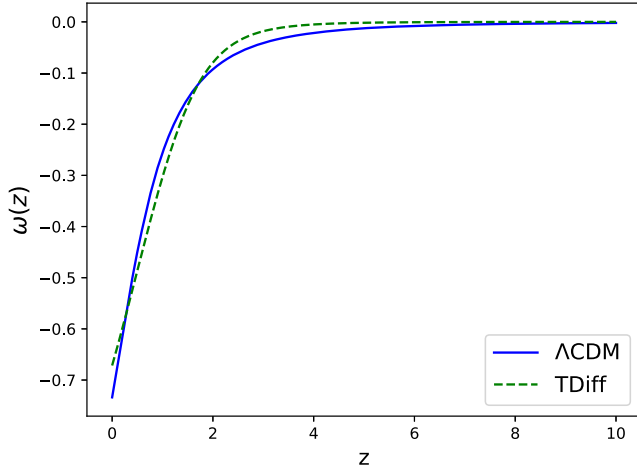8It is important to note that with this definition the cosmic sum rule is only fulfilled at present time.

FIG. 2. Comparison of the equation of state for the dark sector. For the ΛCDM $\omega_{\Lambda\text{CDM}}(z) = (p_{\text{DM}}(z) + p_\Lambda)/(\rho_{\text{DM}}(z) + \rho_\Lambda)$ whereas for the TDiff model $\omega_\phi(z)$ is written in (28). The values of the cosmological parameters can be seen in Table III.

Despite the different behavior of the TDiff effective dark energy equation of state with respect to a cosmological constant, the full dark sector behaves similarly to ΛCDM. Thus in Fig. 2 we compare the dark sector equation of state given by

$$\omega_{\Lambda\text{CDM}}(z) = \frac{p_{\text{DM}}(z) + p_\Lambda}{\rho_{\text{DM}}(z) + \rho_\Lambda} \qquad (56)$$

in ΛCDM with $\omega_\phi(z)$ written in (28) for the TDiff model for the cosmological parameters in Table III.

A. Preferred coordinate time

A unique feature arising from the breaking of the full Diff symmetry is the existence of a preferred coordinate time. In general relativity the lapse function $b(\tau)$ is a pure gauge component in cosmological space-times which can be set to $b(t) = 1$ with a time coordinate transformation. However, in TDiff models $b(\tau)$ is a physical metric component which sets the privileged coordinate time which is related to the cosmological time (that measured by comoving observers) by $b = \frac{dt}{d\tau}$. We can interpret this timescale factor as the rate of change of cosmological time with respect to the privileged time τ, so that, whenever b is constant, means that the two times are essentially the same up to a constant factor. In Fig. 3 we show $b(z)$ for the TDiff model with the cosmological parameters in Table III. We see the constant behavior from the early universe up until the beginning of the accelerated expansion, where it starts to quickly decrease. Notice that the preferred time is unique up to time translations since no time reparametrization was possible via a coordinate transformation satisfying the TDiff condition (A7) while maintaining the spatial coordinates that ensure homogeneity and isotropy.
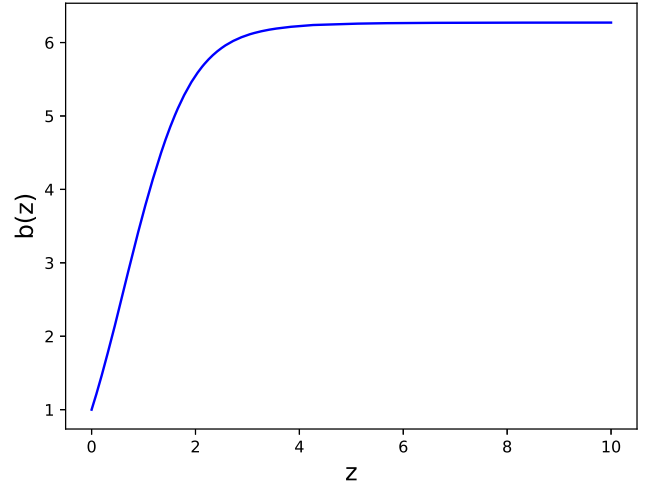

FIG. 3. Time scale factor b as a function of redshift $z = 1/a - 1$ given by the consistency relation (47) that follows from the conservation of the energy-momentum tensor and the equations of motion of the field. The values of the cosmological parameters can be found in Table III.

We can now define the analogue to the usual (space) Hubble rate $H \equiv \frac{\dot{a}}{a}$, but for the lapse function $b(t)$, i.e., a time Hubble rate

$$H_b(a) \equiv \frac{\dot{b}}{b} = \frac{d \ln b}{d \ln a} H(a) = B(a)H(a), \qquad (57)$$

where $B(a)$ can be written in terms of the following combination of $F(g)$
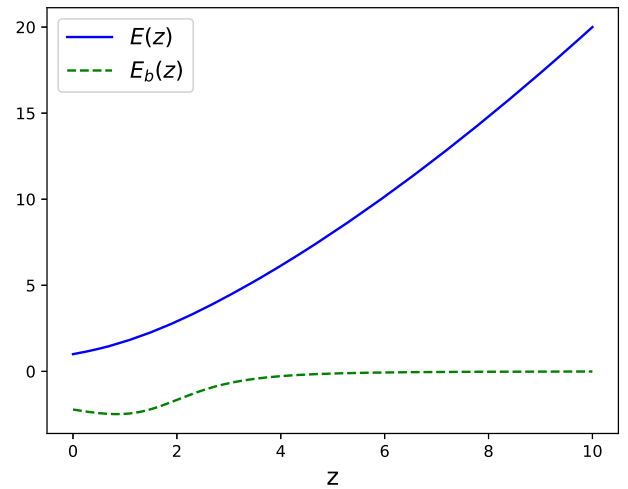
$$B(a) = \frac{3F(3 + 2F)}{1 - F(5 + 2F)}. \qquad (58)$$

FIG. 4. The normalized Hubble rate $E(z) = \frac{1}{H_0}\frac{\dot{a}}{a}$ and $E_b = \frac{1}{H_0}\frac{\dot{b}}{b}$. The values of the cosmological parameters can be found in Table III.

We find that both Hubble rates are related via the function $B(a) \equiv \frac{a}{b}\frac{db}{da}$. This is a consequence of the consistency relation (33), which essentially implies that the timescale factor is a function of the spatial scale factor. We then conclude that b cannot evolve with time unless a does. Nonetheless this is not necessarily true the other way around, as seen in Fig. 3.

Figure 4 shows both Hubble rates in units of H_0 as a function of redshift. $H(z)$ decreases with time whereas $H_b(z)$ goes to zero at large redshifts, so $b(z)$ is constant at the matter dominated era, which is consistent with the discussion above. This is in agreement with the fact that at early times $f(g) = e^{-\beta g} \simeq g^0$, so it behaves as a power law for which $b(a) \propto a^{\frac{3\alpha}{1-\alpha}}$ with $\alpha = 0$, so $b \simeq$ const [7]. The fact that H_b is negative implies that $B(a) < 0$.

IV. DATA AND METHODOLOGY

The model we have just introduced contains the same number of free parameters as ΛCDM. Thus, in the flat ΛCDM, we have at the background level, three free parameters: $(\Omega_M, \Omega_B, H_0)$ where $\Omega_M = \Omega_B + \Omega_{DM}$ contains the contribution from baryons and dark matter.[9] As for the TDiff cosmological model, we also have three free parameters (β, Ω_B, H_0), where the parameter β, somehow, plays a similar role to Ω_M in ΛCDM [see (52)]. It is important to note that in addition to the main cosmological parameters that we have just mentioned we also have to consider the nuisance parameter M which stands for the absolute magnitude in the supernovae data. We shall provide more details about it when we describe the corresponding likelihood. In the following we describe the cosmological datasets employed in this work.

CMB: Instead of considering the full likelihood for Planck 2018 data here we use the CMB distance priors, which for those models that do not depart too much from the ΛCDM predictions at high redshift, turns out to be an efficient way of compressing the information (see Sec. 5.1.6 of [16] for more details). The two distance priors that we utilize here are the shift parameter R and the acoustic length ℓ_a that can be computed from

$$R = \sqrt{\Omega_m H_0^2}(1 + z_*)D_A(z_*), \qquad (59)$$

$$\ell_a = \pi(1 + z_*)\frac{D_A(z_*)}{r_s}. \qquad (60)$$

The above expressions contain the angular distance

---

[9]We consider that the radiation contribution is precisely known from the CMB temperature measurement and the effective number of neutrino species and is given in (38). Since we work in natural units the Hubble parameter is defined by $H_0^{-1} = 2997.9 h^{-1}$ Mpc^{-1}.

$$D_A(z) = \frac{1}{(1+z)}\int_0^z \frac{dz'}{H(z')}, \qquad (61)$$

evaluated at the decoupling redshift z_*, which depends on the free cosmological parameters. In order to get its value we consider the fitting formulas presented in [17]:

$$z_* = 1048[1 + 0.00124\omega_b^{-0.738}][1 + g_1\omega_m^{g_2}], \qquad (62)$$

$$g_1 = \frac{0.0783\omega_b^{-0.238}}{1 + 39.5\omega_b^{0.763}}, \qquad (63)$$

$$g_2 = \frac{0.560}{1 + 21.1\omega_b^{1.81}}, \qquad (64)$$

where $\omega_b \equiv \Omega_B h^2$ and $\omega_m \equiv \Omega_M h^2$. For the TDiff model we do not have the parameter Ω_M, however, since the above formulas are meant to compute $z_* \sim \mathcal{O}(10^3)$, we are allowed to use (52) hence $\Omega_M^{\text{eff}} \equiv \Omega_{DM}^{\text{eff}} + \Omega_B$. The term r_s stands for the radius of the sound horizon

$$r(z) = \int_z^\infty \frac{c_s(z')dz'}{H(z')}, \qquad (65)$$

evaluated at the decoupling epoch $r_s \equiv r(z_*)$ being $c_s(z)$ the speed of sound in the photon-baryon fluid. In addition to the two distance priors we also consider the value of the baryon density ω_b. For the Planck 2018 TT, TE, TE + lowE + lensing [18] data we obtain:

$$\omega_b = 0.02239 \pm 0.00015, \qquad (66)$$

$$\ell_a = 301.529 \pm 0.083, \qquad (67)$$

$$R = 1.7497 \pm 0.0041, \qquad (68)$$

with the corresponding correlation matrix

$$C_{\text{CMB}} = \begin{pmatrix} 1 & -0.2164 & -0.6417 \\ -0.2164 & 1 & 0.3553 \\ -0.6417 & 0.3553 & 1 \end{pmatrix}. \qquad (69)$$

BAO: From isotropic and anisotropic estimators we consider 12 data points, probing the redshif range $0.122 \leq z \leq 2.334$. Here we consider the likelihoods without the growth rates points. The list of measurements utilized in our analysis (for the sake of convenience in some cases we do not show all the decimals of the measurements and the covariance matrices though in the analysis all of them have been considered) can be seen in Table I, and the quantities that appear are, the transverse comoving distance

$$D_M(z) = (1 + z)D_A(z), \qquad (70)$$

TABLE I. BAO measurements.

$z_{\rm eff}$	Measurement	References
0.122	$D_V(r_{d,\rm fid}/r_d)[\rm Mpc] = 539 \pm 17$ [Mpc]	[19]
0.38	$D_M/r_d = 10.2341 \pm 0.1691$	[20]
0.38	$D_H/r_d = 24.9806 \pm 0.7285$	[20]
0.51	$D_M/r_d = 13.3660 \pm 0.2037$	[20]
0.51	$D_H/r_d = 22.3166 \pm 0.5717$	[20]
0.698	$D_M/r_d = 17.8582 \pm 0.3281$	[20,21]
0.698	$D_H/r_d = 19.3258 \pm 0.5327$	[20,21]
0.835	$D_M/r_d = 18.92 \pm 0.51$	[22]
1.48	$D_M/r_d = 30.6876 \pm 0.7983$	[23,24]
1.48	$D_H/r_d = 13.2609 \pm 0.5520$	[23,24]
2.334	$D_M/r_d = 37.5^{+1.2}_{-1.1}$	[25]
2.334	$D_H/r_d = 8.99^{+0.20}_{-0.19}$	[25]

Note: For the data point at $z = 0.122$ the sound horizon size (at the drag epoch), for the fiducial values, computed using (65) is $r_{d,\rm fid} = 148.11$ Mpc [19].

the Hubble radius

$$D_H(z) = \frac{1}{H(z)}, \tag{71}$$

and the angle-averaged distance

$$D_V(z) = [zD_M^2(z)/H(z)]^{1/3}. \tag{72}$$

As usual the observational data points obtained from the BAO analysis are provided as relative distances with respect to the radius of the sound horizon evaluated at the drag epoch $r_d \equiv r(z_d)$. In order to compute the value of z_d, which depends on the value of the cosmological parameters, we make use of the fitting formulas provided in [17]:

$$z_d = 1345 \frac{\omega_m^{0.251}}{1 + 0.659\omega_m^{0.828}}[1 + b_1\omega_b^{b_2}], \tag{73}$$

$$b_1 = 0.313\omega_m^{-0.419}[1 + 0.607\omega_m^{0.674}], \tag{74}$$

$$b_2 = 0.238\omega_m^{0.223}. \tag{75}$$

Finally we provide the corresponding covariance matrices.

The covariance matrix between measurements for the BOSS Galaxy data [20] is given by

$$\rm Cov_{BOSS\text{-}Galaxy} = \begin{pmatrix} 0.02860520 & -0.04939281 & 0.01489688 & -0.01387079 \\ -0.04939281 & 0.5307187 & -0.02423513 & 0.01767087 \\ 0.01489688 & -0.02423513 & 0.04147534 & -0.04873962 \\ -0.01387079 & 0.01767087 & -0.04873962 & 0.3268589 \end{pmatrix}. \tag{76}$$

For the two data-points obtained with eBOSS LRG data [20,21] the covariance matrix is

$$\rm Cov_{eBOSS\text{-}LRG} = \begin{pmatrix} 0.1076634 & -0.0583182 \\ -0.0583182 & 0.2838176 \end{pmatrix} \tag{77}$$

whereas for the eBOSS Quasar data [23,24]

$$\rm Cov_{eBOSS\text{-}Quasar} = \begin{pmatrix} 0.63731604 & 0.1706891 \\ 0.1706891 & 0.30468415 \end{pmatrix}. \tag{78}$$

Finally the covariance matrix for the Lyα forest data is given by

$$\rm Cov_{Ly\alpha} = \begin{pmatrix} 1.3225 & -0.1009 \\ -0.1009 & 0.0380 \end{pmatrix}. \tag{79}$$

Cosmic chronometers: We include in our analysis 32 measurements of $H(z_i)$, covering the redshift range $0.07 \le z \le 1.965$, obtained with the differential age technique. For those data points that are correlated with each other (see [26] for more details) the corresponding covariance matrix can be computed with the script provided here.[10] The list of measurements of the Hubble parameter can be seen in Table II. Those that appear without the corresponding error bars are the ones that are correlated with each other.

SNIa: We employ the data from the Pantheon + &SH0ES compilation [32,33] which contains 1701 light curves obtained from 1550 distinct SNIa with redshifts in the range $0.001 \le z \le 2.26$. Within these 1550 SNIa there are 42 SNIa (with 77 light curves associated) in 37 Cepheid host galaxies, whose distance moduli have been obtained by measuring the characteristic period-luminosity relation of these variable stars. These measurements have been carried out by the SH0ES collaboration [34]. The fact of using the 77 distance moduli provided by the SH0ES team turns out to be fundamental to break the well-known degeneracy between the Hubble parameter H_0 and the absolute magnitude, which here we denote by M. Let us provide some specifics of the formulation used in the corresponding likelihood.

---

[10]https://gitlab.com/mmoresco/CCcovariance/-/blob/master/examples/CC_covariance.ipynb.

TABLE II. Hubble parameter data.

z	$H(z)$ (km s^{-1} Mpc^{-1})	References
0.07	69.0 ± 19.6	[27]
0.09	69.0 ± 12.0	[28]
0.12	68.6 ± 26.2	[27]
0.17	83.0 ± 8.0	[28]
0.2	72.9 ± 29.6	[27]
0.27	77.0 ± 14.0	[28]
0.28	88.8 ± 36.6	[27]
0.4	95.0 ± 17.0	[28]
0.47	89.0 ± 50.0	[29]
0.48	97.0 ± 62.0	[30]
0.75	98.8 ± 33.6	[31]
0.88	90.0 ± 40.0	[30]
0.9	117.0 ± 23.0	[28]
1.3	168.0 ± 17.0	[28]
1.43	177.0 ± 18.0	[28]
1.53	140.0 ± 14.0	[28]
1.75	202.0 ± 40.0	[28]
0.1791	74.91	[26]
0.1993	74.96	[26]
0.3519	82.78	[26]
0.3802	83.0	[26]
0.4004	76.97	[26]
0.4247	87.08	[26]
0.4497	92.78	[26]
0.4783	80.91	[26]
0.5929	103.8	[26]
0.6797	91.6	[26]
0.7812	104.5	[26]
0.8754	125.1	[26]
1.037	153.7	[26]
1.363	160.0	[26]
1.965	186.5	[26]

The basic observable is the apparent magnitude m which can be expressed as follows

$$m(z_{\mathrm{HD}}, z_{\mathrm{HEL}}) = \mu(z_{\mathrm{HD}}, z_{\mathrm{HEL}}) + M, \qquad (80)$$

being μ the distance modulus

$$\mu(z_{\mathrm{HD}}, z_{\mathrm{HEL}}) = 25 + 5 \log_{10}\left(\frac{\tilde{d}_L(z_{\mathrm{HD}}, z_{\mathrm{HEL}})}{1 \text{ Mpc}}\right), \quad (81)$$

where the quantity $\tilde{d}_L(z_{\mathrm{HD}}, z_{\mathrm{HEL}})$ can be understood as a corrected luminosity distance. Therefore we have:

$$\tilde{d}_L(z_{\mathrm{HD}}, z_{\mathrm{HEL}}) = \left(\frac{1 + z_{\mathrm{HEL}}}{1 + z_{\mathrm{HD}}}\right) d_L(z_{\mathrm{HD}}), \qquad (82)$$

being the expression for the luminosity distance in a spatially flat universe the usual one

$$d_L(z_{\mathrm{HD}}) = \frac{(1 + z_{\mathrm{HD}})}{H_0} \int_0^{z_{\mathrm{HD}}} \frac{dz'}{E(z')}. \qquad (83)$$

In the above expressions z_{HD} stands for the Hubble diagram redshift whereas z_{HEL} represents the heliocentric redshift. When the light curve considered is one of the 77 mentioned before (they are labeled with IS_CALIBRATOR = 1 in the data file) instead of using (81) to compute the distance modulus, we consider SH0ES' measurement for this quantity. This constraints greatly the value of the absolute magnitude M (which in our analysis has the role of a nuisance parameter) thus breaking the existing degeneracy between $H_0 - M$.

We consider the following joint χ^2-function

$$\chi_{\mathrm{tot}}^2 = \chi_{\mathrm{CMB}}^2 + \chi_{\mathrm{BAO}}^2 + \chi_{\mathrm{H}}^2 + \chi_{\mathrm{SNIa}}^2 \qquad (84)$$

in order to study the performance of the ΛCDM and TDiff cosmological models when they are confronted with the dataset previously described. The dataset considered in (84) will be referred to as baseline. We explore the parameter-space that characterizes each of the models with the Markov chain Monte Carlo analysis, making use of the Metropolois-Hastings algorithm [35,36]. Once the converged chains have been obtained we utilize the GetDist code [37] to obtain the mean values of the different cosmological parameters, the associated confidence intervals and the posterior distributions. When exploring the parameter-space we have set the following priors for the three common parameters $0.01 < \Omega_b < 0.1$, $40 < H_0 \, [\mathrm{km/s/Mpc}] < 100$ and $-20 < M < -18$. In the ΛCDM case we have considered $0.1 < \Omega_m < 0.5$ whereas for the TDiff model $1.7 < \beta < 2.3$. We want to compare the performance of the ΛCDM model and the TDiff model, therefore in this work we use the deviance information criterion (DIC) [38], whose value can be computed from

$$\mathrm{DIC} = \chi^2(\bar{\theta}) + 2p_D. \qquad (85)$$

In the above expression, $p_D = \overline{\chi^2} - \chi^2(\bar{\theta})$ stands for the effective number of parameters, $\overline{\chi^2}$ is the mean value of the χ^2-function and $\bar{\theta}$ contains the mean value of the free parameters. We define the difference with respect to the ΛCDM model as follows

$$\Delta\mathrm{DIC} = \mathrm{DIC}_{\Lambda\mathrm{CDM}} - \mathrm{DIC}_{\mathrm{TDiff}}, \qquad (86)$$

as a consequence if we obtain positive values of ΔDIC means that the TDiff model is favored over the ΛCDM models whereas negative values indicate the other way around. Having defined the difference in the DIC values as in (86), according to the usual standards if we find values $0 \leq \Delta\mathrm{DIC} < 2$ we say there is *weak* evidence in favor of the TDiff model. If we get values $2 \leq \Delta\mathrm{DIC} < 6$ we speak

of *positive* evidence whereas values $6 \leq \Delta\text{DIC} < 10$ point out to *strong* evidence in favor of the TDiff. Finally, finding values $\Delta\text{DIC} > 10$ would allow us to claim *very strong* evidence. As we mentioned before negative values would indicate evidence in favor of the standard model.

In order to complement the DIC we also make use of the Bayesian evidence which has been computed following the procedure detailed in [39]. Here we define the Bayes' ratio as

$$\mathcal{B} \equiv \frac{E_{\text{TDiff}}}{E_{\Lambda\text{CDM}}}, \qquad (87)$$

where E stands for the Bayesian evidence. With the above definition, and as with the DIC, positive values indicate that the TDiff model is favored over the ΛCDM model with different levels of significance. Therefore if $\ln \mathcal{B} \leq 1$ there is *inconclusive* evidence, for $1 < \ln \mathcal{B} \leq 2.5$ we get *moderate* evidence whereas if we obtain $2.5 < \ln \mathcal{B} \leq 5$ we speak of *strong* evidence. Finally if we find values $\ln \mathcal{B} > 5$ we are allowed to claim *very strong* evidence in favor of the TDiff model. For negative values of $\ln \mathcal{B}$ is the other way around.

V. RESULTS

The best-fit values and the corresponding 68% confidence intervals, obtained after considering the baseline dataset [see Eq. (84)], can be found in Table III and in Figs. 5 and 6. We see that the TDiff model provides an excellent fit to the considered dataset with a minimum χ^2 below that of ΛCDM with same number of free parameters. As a matter of fact $\Delta\text{DIC} = 10.39$ indicates *very strong* evidence whereas $\ln \mathcal{B} = 4.02$ indicates *strong* evidence in favor of the TDiff model when it is confronted against the ΛCDM. The main difference appears in the mean value of the Hubble parameter which is larger than in the ΛCDM and with similar error bars. As we will show below, this will mainly explain the better fit to the complete dataset.

TABLE III. Mean values with the 68% confidence interval for the cosmological parameters considered obtained by analyzing the Baseline dataset [see Eq. (84)]. We also show the minimum value of the χ^2-function, the incremental value of the DIC and the value of $\ln \mathcal{B}$.

	Baseline	
	ΛCDM	TDiff
Ω_B	0.04775 ± 0.00042	0.04647 ± 0.00035
Ω_M	0.3012 ± 0.0049	$\cdots$
H_0 [km/s/Mpc]	68.82 ± 0.38	69.46 ± 0.34
β	$\cdots$	2.045 ± 0.027
M	-19.398 ± 0.011	-19.369 ± 0.010
$\chi^2_{\min}$	1338.34	1327.97
ΔDIC	$\cdots$	10.39
$\ln \mathcal{B}$	$\cdots$	4.02

As commented before, at high redshift, the TDiff scalar field mimics the nonrelativistic matter behavior as it is clear from (51) and consequently the effective matter density parameter at that time is $\Omega_M^{\text{eff}} = \Omega_{\text{DM}}^{\text{eff}} + \Omega_B = 0.3005 \pm 0.0043$ (computed as a derived parameter obtained with the Baseline dataset), which can be compared with the ΛCDM value $\Omega_M = 0.3012 \pm 0.0049$. Therefore, the behavior of the TDiff model is very similar to the ΛCDM model at high-redshift, when the contribution from dark energy is negligible.

On the other hand if we want to study the behavior of the TDiff model at late times, we may look at the equation of state parameter, which at present time, takes the value $\omega_\phi(z = 0) = -0.6746 \pm 0.0029$. The equivalent quantity for the ΛCDM model would be $\omega_{\Lambda\text{CDM}}(z = 0) = -0.7383 \pm 0.0044$ with $\omega_{\Lambda\text{CDM}}$ defined in (56). The low-redshift evolution of both parameters can be seen in Fig. 2. The fact that the value in the ΛCDM model is, in absolute value, greater than the value in the TDiff model indicates that the behavior of the scalar field is quintessencelike. This is confirmed thanks to the effective equation of state parameter for the dark energy component defined in Eq. (55), whose present value $\omega_{\text{DE}}^{\text{eff}}(z = 0) = -0.9156 \pm 0.0016$ lies in the quintessence region. As shown in Fig. 1, the TDiff model evolves from a phantom effective dark energy equation of state $\omega_{\text{DE}}^{\text{eff}}(z) = -2$ at high redshift to a quintessencelike value at present.

We also find some differences between the models when it comes to the redshift value that marks the transition from a decelerated to an accelerated expanding universe. Whereas for the ΛCDM we have $z_t \simeq 0.668$ for the TDiff we get $z_t \simeq 0.794$ and the corresponding value of the $b(a)$ parameter $b_t \simeq 3.1314$. In Fig. 3 we show the behavior of $b(z)$ which is constant in the matter dominated era, being this constant value $b(z \gg 1) \simeq \sqrt{1 + 2\beta}\, e^{\frac{\beta}{2}} \simeq 6.272$.

A. The H_0-tension

The persisting mismatch between the value obtained by the Planck collaboration ($H_0 = 67.36 \pm 0.54$ km/s/Mpc from TT, TE, EE + lowE + lensing data [18]) and the SH0ES measurement ($H_0 = 73.04 \pm 1.04$ km/s/Mpc [34] which hereafter will be denoted by H_0^{SH0ES}), obtained with the inverse cosmic distance ladder method, has become a central topic of study in cosmology in recent years. In order to calculate the tension between two given values we utilize the following estimator

$$T_{H_0} = \frac{\left| H_0^{(1)} - H_0^{(2)} \right|}{\sqrt{\sigma_{(1)}^2 + \sigma_{(2)}^2}}. \qquad (88)$$

Therefore the tension between the mentioned values reaches the astonishing level of $T_{H_0} \simeq 4.85\sigma$. At this stage it is still not clear whether the tension is somehow caused
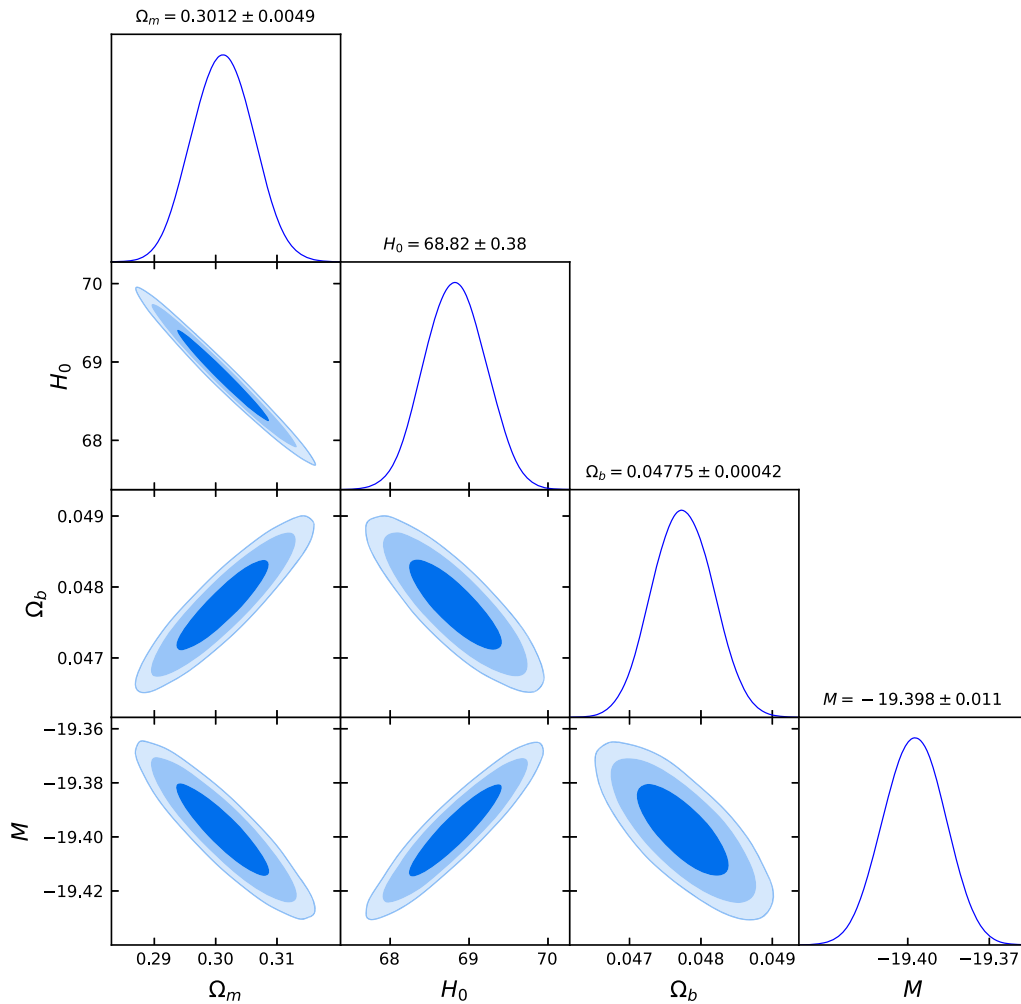
FIG. 5.   For the ΛCDM model contour plots at 1σ, 2σ and 3σ confidence level, as well as, the one-dimensional posterior distributions for the Baseline dataset. The H_0 parameter is expressed in km/s/Mpc units.

by some sort of unknown systematic or if it is actually the clearest hint we have so far of physics beyond the standard model.

This section is specifically aimed to check how the TDiff model deals with the H_0-tension. It has been argued [40] that no low-redshift solution can completely solve the tension. The authors consider a very flexible parametrization of the equation of the state parameter to prove that the 1-dimensional posterior distribution of the H_0 parameter ($H_0 = 68.08 \pm 0.97$ km/s/Mpc), obtained from a CMB + BAO + SNIa (the SNIa data do not contain SH0ES measurement unlike the one we consider here) dataset, does not overlap with SH0ES' measurement posterior distribution.

For the sake of comparison we have tested the TDiff model with a combination of data CMB + BAO + SNIa*, where the * indicates that in this occasion the SNIa data do not contain the SH0ES contribution. Regarding the Hubble parameter we get the following result $H_0 = 68.95 \pm 0.37$ km/s/Mpc, which is perfectly compatible with the value provided in [40].

If we have a look at Tables IV and V we can see the results obtained when first only the CMB and then only the SNIa data (in addition we consider a model-independent BBN prior for the density of baryons $\omega_b = 0.02244 \pm 0.00069$ [41] determined by D/H abundances) are considered, whereas in Table VI we provide the results when both of these datasets are jointly considered. In Table IV we can see that for the TDiff model we get $H_0 = 69.49 \pm 0.51$ km/s/Mpc which is in 3.1σ tension with H_0^{SH0ES}, representing a clear reduction with respect to the result obtained for the ΛCDM ($H_0 = 67.72 \pm 0.57$ km/s/Mpc showing a discrepancy of 4.5σ with the SH0ES measurement). On the other hand, when only the likelihood for the SNIa data is taken into account we get almost the same results for both models (see Table V). It is when we analyze both datasets together (results provided in Table VI) when we are able to appreciate the different performance of the two models when it comes to fitting the data. We obtain Δ DIC = 15.80 and $\ln \mathcal{B} = 6.90$ which according to the statistical standards indicates a *very strong* evidence in
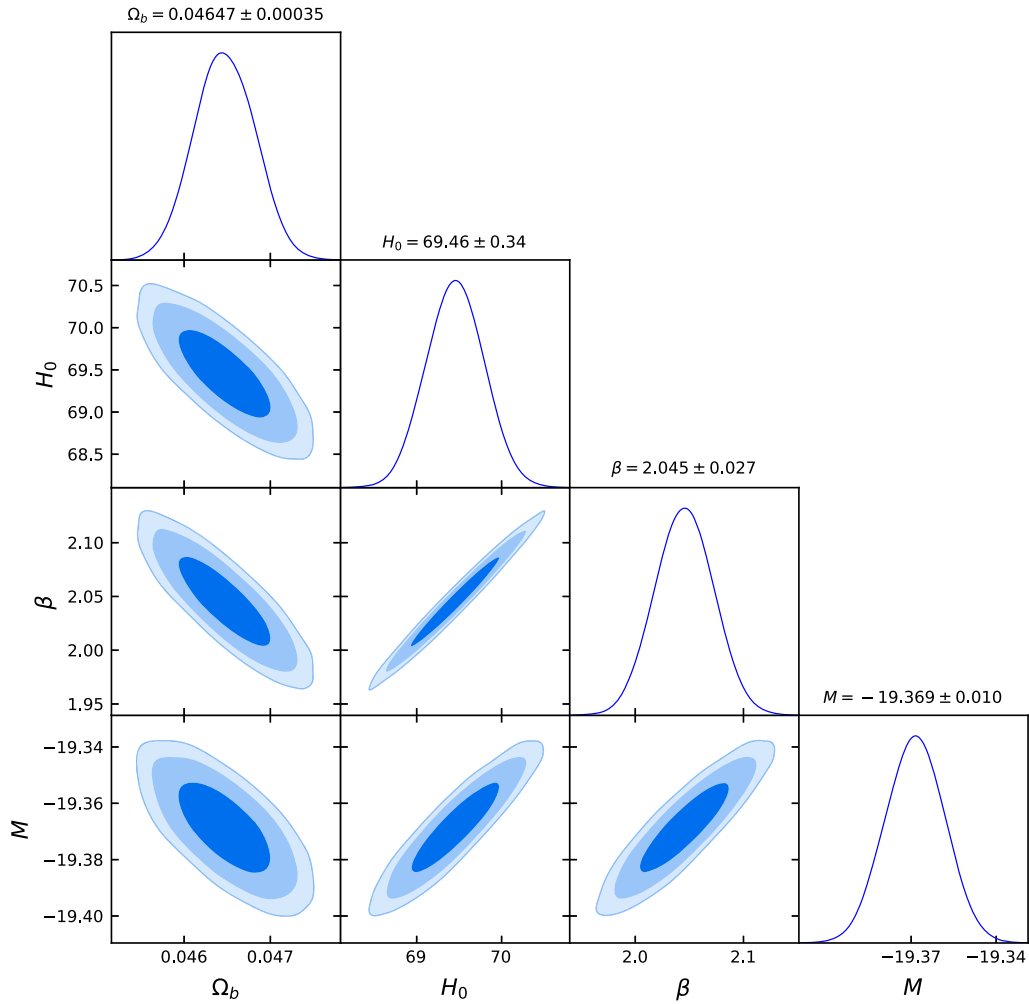
FIG. 6. Same as in Fig. 5 but for the TDiff model.

favor of the TDiff model when it is compared with the standard model. In Figs. 7 and 8 we display the contour plots for the ΛCDM and the TDiff models respectively. While for the standard model there are panels where the contours do not overlap at more than 3σ c.l., which is of course a reflection of the previously presented H_0-tension, in the case of the TDiff we observe that the model shows

greater capacity to fit both datasets, CMB and SNIa, simultaneously. It is worth noticing that the TDiff model can alleviate the H_0-tension without including extra parameters, with respect to the ΛCDM model, which normally increases the size of the error bars thus reducing

TABLE IV. Mean values with the 68% confidence interval for the cosmological parameters when only CMB data are considered.

	CMB	
	ΛCDM	TDiff
Ω_B	0.04882 ± 0.00062	0.04638 ± 0.00049
Ω_M	0.3158 ± 0.0078	$\cdots$
H_0 [km/s/Mpc]	67.72 ± 0.57	69.49 ± 0.51
β	$\cdots$	2.049 ± 0.041
$\chi^2_{\min}$	0	0
ΔDIC	$\cdots$	-0.97
$\ln \mathcal{B}$	$\cdots$	-0.09

TABLE V. Mean values with the 68% confidence interval for the cosmological parameters when only SNIa data and the prior $\omega_b = 0.02244 \pm 0.00069$ [41] are considered.

	SNIa + prior on ω_b	
	ΛCDM	TDiff
Ω_B	0.0414 ± 0.0019	0.0415 ± 0.0019
Ω_M	0.329 ± 0.020	$\cdots$
H_0 [km/s/Mpc]	73.7 ± 1.1	73.6 ± 1.1
β	$\cdots$	$1.92^{+0.10}_{-0.15}$
M	-19.244 ± 0.033	-19.243 ± 0.032
$\chi^2_{\min}$	1277.13	1277.48
ΔDIC	$\cdots$	0.23
$\ln \mathcal{B}$	$\cdots$	-0.16

TABLE VI. Mean values with the 68% confidence interval for the cosmological parameters when SNIa + CMB data are considered.

	CMB + SNIa	
	ΛCDM	TDiff
Ω_B	0.04770 ± 0.00053	0.04587 ± 0.00044
Ω_M	0.3007 ± 0.0064	$\cdots$
H_0 [km/s/Mpc]	68.86 ± 0.49	70.10 ± 0.45
β	$\cdots$	2.098 ± 0.036
M	-19.396 ± 0.014	-19.351 ± 0.013
$\chi^2_{\min}$	1310.06	1294.13
ΔDIC	$\cdots$	15.80
$\ln \mathcal{B}$	$\cdots$	6.90

the tension. In fact, they are smaller than in the standard model which means that the softening of the tension actually comes from an increase of the mean value. Additionally, this goes hand-in-hand with a fit of

observational data comparable, if not better, to the one of the ΛCDM model, something that despite the number of cosmological models studied in the literature [10], is not easy to achieve.

Even in the light of these promising results we are not claiming that the H_0-tension is solved within the context of the TDiff cosmological model. When CMB data are considered the level of tension, with respect to the local measurement H_0^{SH0ES}, is still $\sim 3\sigma$ which although it is not as alarming as the $\sim 5\sigma$ tension found for the ΛCDM when the full Planck 2018 TT, TE, EE + lowE + lensing likelihood is analyzed, it is still quite high and consequently it cannot be ignored. It is also important to remember that in this work we have used an approximation for the CMB likelihood [see (66) and (69)] therefore some variations in the cosmological parameter constraints may be expected when considering the full likelihood, something that the authors are currently studying. All in all, we find that the TDiff model presents an interesting flexibility when it
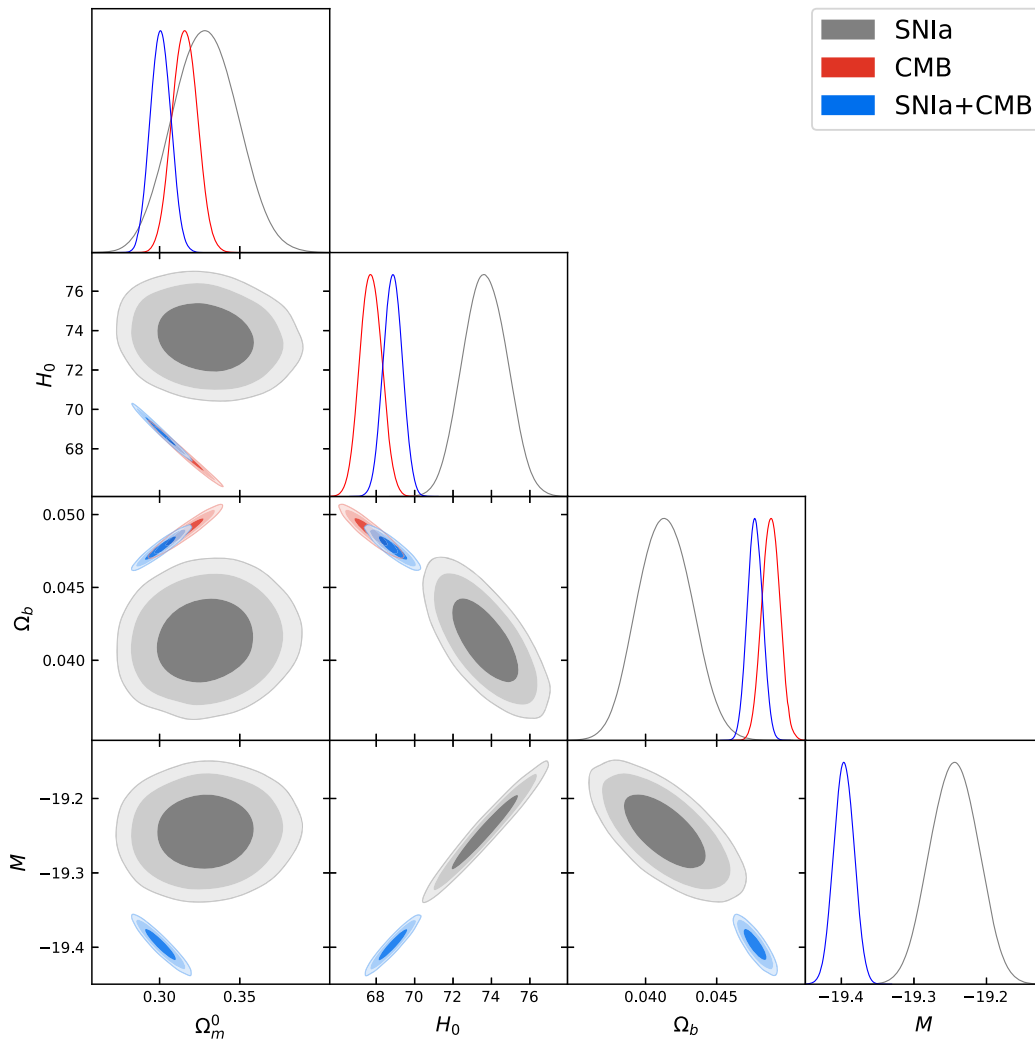

FIG. 7. For the ΛCDM model contour plots at 1σ, 2σ, and 3σ confidence level for the SNIa + prior on ω_b, CMB and SNIa + CMB data. The H_0 parameter is expressed in km/s/Mpc units.
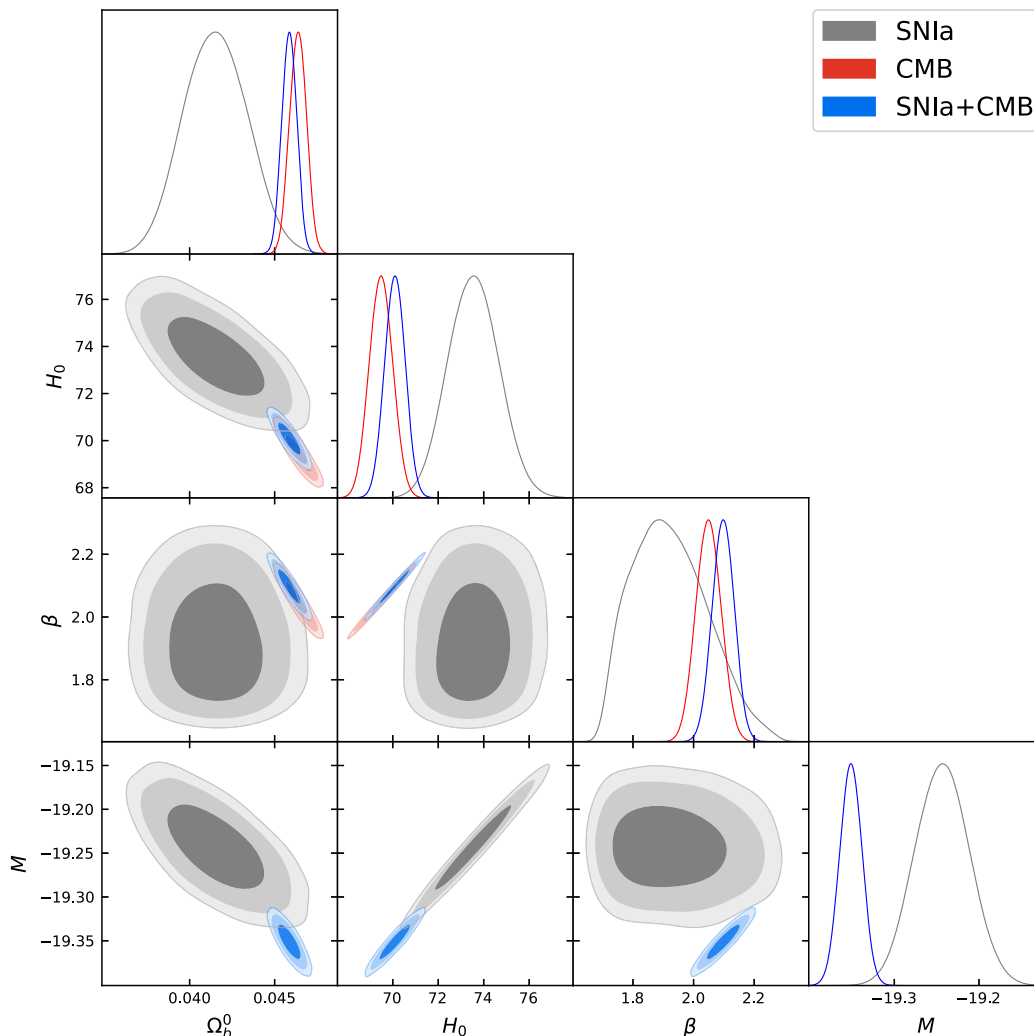
FIG. 8.   Same as in Fig. 7 but for the TDiff model.

comes to push up the value of the H_0 parameter, thus loosening the discrepancy with the H_0^{SH0ES} measurement but more detailed studies are needed in order to confirm these results.

VI. CONCLUSIONS

In this work we have presented a unified model for the dark sector with a simple canonical kinetic term in the action. This theory is based on a scalar field ϕ that explicitly breaks the full diffeomorphism invariance of the action down to transverse diffeomorphisms, i.e., the action (11) is invariant under coordinate transformations that do not change the determinant of the metric tensor. The function characterizing the Diff breaking is a simple exponential $f(g) = e^{-\beta g}$. The model has the same number of free parameters as ΛCDM, being the common ones Ω_B, H_0 and the nuisance parameter M and where the β parameter replaces the Ω_M parameter of ΛCDM.

Unlike General Relativity, in the TDiff case there are two physical scale factors in the metric tensor at the background level, namely: $a(\tau)$ and $b(\tau)$, being τ a privileged time, established by the TDiff symmetry and related with the cosmological time t through $b = dt/d\tau$. This is so because no time reparametrizations with fixed spatial coordinates (to maintain homogeneity and isotropy) are allowed by the symmetry. Even at the background level, the TDiff time τ differs from the time t that a comoving observer would measure, so that for a process that takes a fixed $\Delta\tau$ amount of time, since b decreases with cosmological time t, the corresponding Δt becomes smaller. This can be thought of as some kind of time dilation of τ with respect to t.

As stated previously we consider a unified fluid playing the role of both dark matter and dark energy, therefore, the expression chosen for $f(g)$ is such that the equation of state parameter (28) of the fluid interpolates between a matter-type behavior and a cosmological constant-type one. In fact, at the background level we can effectively separate the contribution from the scalar field into two components,

one mimicking the evolution of the nonrelativistic matter and another one behaving as if it were a dark energy component which evolves from a phantom phase in the early universe to a quintessencelike behavior at present. Other forms of the $f(g)$ function can be analyzed, but the simple exponential expression considered in this work already shows the flexibility of TDiff models to describe the dark sector without introducing additional parameters.

Previous works [6–8,14] aim at presenting viable models on cosmological backgrounds with this reduced TDiff symmetry, however, this is the first time that a consistent model is actually compared with experiment and constraints on its parameters are presented. We have considered different datasets in order to test the model in different scenarios. The results obtained after analyzing the baseline dataset, composed by the chain of data CMB + BAO + $H(z)$ + SNIa, can be seen in Table III and in Figs. 5 and 6. Encouraging signals are gathered indicating that the TDiff model can surpass the performance of the standard ΛCDM model when it comes to fitting the data. However, these promising results are to be confirmed by including in the analysis the full likelihood for the CMB data and by considering the perturbation equations. The potential modification in the evolution of perturbations could affect some of the observables considered in the analysis. In particular, the CMB distance priors and BAO scales could be affected *a priori*. Those observables are determined by the acoustic scale at the time of recombination (drag epoch), however at high redshift, the TDiff scalar behaves exactly as a matter fluid, so that we do not expect any modification in the evolution of perturbations in the radiation or matter eras with respect to ΛCDM. Nevertheless, a confrontation with growth rate data or the full matter power spectrum would require a more detailed determination of the evolution of perturbations at low redshift which could deviate from ΛCDM.

We have also delved into the study of the well-known H_0-tension. Interestingly we observe that the TDiff model is able to alleviate the tension, when compared with the ΛCDM model, not stretching the error bars but rather pushing the mean value of Hubble parameter toward higher values.

In light of the results obtained in this work we conclude that the general class of transverse diffeomorphism invariant models not only present an appealing theoretical framework, where there may be a way out of the cosmological constant problem, but also provides an interesting alternative to explain the cosmological data and what is more to alleviate some tensions that affect the ΛCDM model.

ACKNOWLEDGMENTS

APPENDIX: TDiff INVARIANT SCALARS

Let us consider an infinitesimal general coordinate transformation

$$\hat{x}^\mu = x^\mu + \xi^\mu(x). \tag{A1}$$

The corresponding transformation law for the metric tensor reads

$$\hat{g}_{\mu\nu}(\hat{x}) = \frac{\partial x^\alpha}{\partial \hat{x}^\mu}\frac{\partial x^\beta}{\partial \hat{x}^\nu} g_{\alpha\beta}(x), \tag{A2}$$

so that its determinant transforms as a tensor density

$$\hat{g}(\hat{x}) = \left| \det\left(\frac{\partial x^\alpha}{\partial \hat{x}^\mu}\right)\right|^2 g(x). \tag{A3}$$

At an infinitesimal level, by using the identity $\det(\mathbb{1} + A) = 1 + \text{tr}(A) + \mathcal{O}(A^2)$, we get

$$\left|\det\left(\frac{\partial x^\alpha}{\partial \hat{x}^\mu}\right)\right|^2 = \left|\det\left(\delta^\alpha_\mu - \frac{\partial \xi^\alpha}{\partial \hat{x}^\mu}\right)\right|^2 = 1 - 2\partial_\mu\xi^\mu(x) + \mathcal{O}(\xi^2), \tag{A4}$$

where we have also made use of the fact that the derivatives of $\xi^\mu(x)$ with respect to the new coordinates $\hat{x}^\mu$ can be replaced with the derivatives with respect to the old coordinates to linear order in $\xi^\mu(x)$. This means that since

$$\hat{g}(\hat{x}) = (1 - 2\partial_\mu\xi^\mu)g(x), \tag{A5}$$

$$d^4\hat{x} = (1 + \partial_\mu\xi^\mu)d^4x, \tag{A6}$$

for any coordinate transformation that satisfies

$$\partial_\mu\xi^\mu = 0, \tag{A7}$$

then any action term of the form

$$S = \int d^4x f(g)\mathcal{L}, \tag{A8}$$

where $f(g)$ is an arbitrary function of the metric determinant and $\mathcal{L}$ is a scalar function of the matter fields, its derivatives and the metric tensor, is invariant under these transformations. Coordinate transformations that satisfy the condition (A7) are referred to as transverse diffeomorphisms.

Thus, to lowest order in metric derivatives, the most general TDiff invariant action up to quadratic terms in derivatives of a real scalar field reads [6,7]

$$S_\phi = \int d^4x \mathcal{L} = \int d^4x \left(\frac{1}{2} f_K(g) g^{\mu\nu} \partial_\mu \phi \partial_\nu \phi - f_V(g) V(\phi) \right), \tag{A9}$$

where $f_K(g)$ and $f_V(g)$ are arbitrary functions of the metric determinant. Notice that in principle, other (nonminimal) terms could be included involving derivatives of the metric tensor, but we will limit ourselves to the simplest minimal couplings.

[1] C. M. Will, The confrontation between general relativity and experiment, Living Rev. Relativity **17**, 4 (2014).

[2] S. Weinberg, *Gravitation and Cosmology: Principles and Applications of the General Theory of Relativity* (John Wiley and Sons, New York, 1972).

[3] H. Velten and T. R. P. Caramês, To conserve, or not to conserve: A review of nonconservative theories of gravity, Universe **7**, 38 (2021).

[4] A. Einstein, Spielen Gravitationsfelder im Aufbau der materiellen Elementarteilchen eine wesentliche Rolle?, Sitzungsber. Preuss. Akad. Wiss. Berlin (Math. Phys.) **1919**, 349 (1919).

[5] G. F. R. Ellis, H. van Elst, J. Murugan, and J.-P. Uzan, On the trace-free Einstein equations as a viable alternative to general relativity, Classical Quantum Gravity **28**, 225007 (2011).

[6] E. Álvarez, A. F. Faedo, and J. López-Villarejo, Transverse gravity versus observations, J. Cosmol. Astropart. Phys. 07 (2009) 002.

[7] A. L. Maroto, TDiff invariant field theories for cosmology, arXiv:2301.05713.

[8] D. Jaramillo-Garrido, A. L. Maroto, and P. Martín-Moruno, TDiff in the dark: Gravity with a scalar field invariant under transverse diffeomorphisms, arXiv:2307.14861.

[9] A. Y. Kamenshchik, U. Moschella, and V. Pasquier, An alternative to quintessence, Phys. Lett. B **511**, 265 (2001).

[10] E. Di Valentino, O. Mena, S. Pan, L. Visinelli, W. Yang, A. Melchiorri, D. F. Mota, A. G. Riess, and J. Silk, In the realm of the Hubble tension—A review of solutions, Classical Quantum Gravity **38**, 153001 (2021).

[11] H. Sandvik, M. Tegmark, M. Zaldarriaga, and I. Waga, The end of unified dark matter?, Phys. Rev. D **69**, 123524 (2004).

[12] J. Ren and X.-H. Meng, Cosmological model with viscosity media (dark fluid) described by an effective equation of state, Phys. Lett. B **633**, 1 (2006).

[13] R. J. Scherrer, Purely kinetic k-essence as unified dark matter, Phys. Rev. Lett. **93**, 011301 (2004).

[14] A. G. Bello-Morales and A. L. Maroto, Cosmology in gravity models with broken diffeomorphisms, arXiv:2308.00635.

[15] L. Heisenberg, H. Villarrubia-Rojo, and J. Zosso, Can late-time extensions solve the H_0 and σ_8 tensions?, Phys. Rev. D **106**, 043503 (2022).

[16] P. A. R. Ade *et al.* (Planck Collaboration), Planck 2015 results. XIV. Dark energy and modified gravity, Astron. Astrophys. **594**, A14 (2016).

[17] W. Hu and N. Sugiyama, Small scale cosmological perturbations: An analytic approach, Astrophys. J. **471**, 542 (1996).

[18] N. Aghanim *et al.* (Planck Collaboration), Planck 2018 results. VI. Cosmological parameters, Astron. Astrophys. **641**, A6 (2020); **652**, C4(E) (2021).

[19] P. Carter, F. Beutler, W. J. Percival, C. Blake, J. Koda, and A. J. Ross, Low redshift baryon acoustic oscillation measurement from the reconstructed 6-degree field galaxy survey, Mon. Not. R. Astron. Soc. **481**, 2371 (2018).

[20] H. Gil-Marin *et al.*, The completed SDSS-IV extended Baryon Oscillation Spectroscopic Survey: Measurement of the BAO and growth rate of structure of the luminous red galaxy sample from the anisotropic power spectrum between redshifts 0.6 and 1.0, Mon. Not. R. Astron. Soc. **498**, 2492 (2020).

[21] J. E. Bautista *et al.*, The completed SDSS-IV extended Baryon Oscillation Spectroscopic Survey: Measurement of the BAO and growth rate of structure of the luminous red galaxy sample from the anisotropic correlation function between redshifts 0.6 and 1, Mon. Not. R. Astron. Soc. **500**, 736 (2020).

[22] T. M. C. Abbott *et al.* (DES Collaboration), Dark Energy Survey Year 3 results: Cosmological constraints from galaxy clustering and weak lensing, Phys. Rev. D **105**, 023520 (2022).

[23] J. Hou *et al.*, The completed SDSS-IV extended Baryon Oscillation Spectroscopic Survey: BAO and RSD measurements from anisotropic clustering analysis of the quasar sample in configuration space between redshift 0.8 and 2.2, Mon. Not. R. Astron. Soc. **500**, 1201 (2020).

[24] R. Neveux *et al.*, The completed SDSS-IV extended Baryon Oscillation Spectroscopic Survey: BAO and RSD measurements from the anisotropic power spectrum of the quasar sample between redshift 0.8 and 2.2, Mon. Not. R. Astron. Soc. **499**, 210 (2020).

[25] H. du Mas des Bourboux *et al.*, The completed SDSS-IV extended baryon oscillation spectroscopic survey: Baryon acoustic oscillations with Lyα Forests, Astrophys. J. **901**, 153 (2020).

[26] M. Moresco, R. Jimenez, L. Verde, A. Cimatti, and L. Pozzetti, Setting the stage for cosmic chronometers. II. Impact of stellar population synthesis models systematics and full covariance matrix, Astrophys. J. **898**, 82 (2020).

[27] C. Zhang, H. Zhang, S. Yuan, T.-J. Zhang, and Y.-C. Sun, Four new observational $H(z)$ data from luminous red galaxies in the Sloan Digital Sky Survey data release seven, Res. Astron. Astrophys. **14**, 1221 (2014).

[28] J. Simon, L. Verde, and R. Jimenez, Constraints on the redshift dependence of the dark energy potential, Phys. Rev. D **71**, 123001 (2005).

[29] A. L. Ratsimbazafy, S. I. Loubser, S. M. Crawford, C. M. Cress, B. A. Bassett, R. C. Nichol, and P. Väisänen, Age-dating luminous red galaxies observed with the Southern African Large Telescope, Mon. Not. R. Astron. Soc. **467,** 3239 (2017).

[30] D. Stern, R. Jimenez, L. Verde, M. Kamionkowski, and S. A. Stanford, Cosmic chronometers: Constraining the equation of state of dark energy. I: H(z) measurements, J. Cosmol. Astropart. Phys. 02 (2010) 008.

[31] N. Borghi, M. Moresco, and A. Cimatti, Toward a better understanding of cosmic chronometers: A new measurement of H(z) at z ∼ 0.7, Astrophys. J. Lett. **928,** L4 (2022).

[32] D. Scolnic *et al.*, The Pantheon+ analysis: The full dataset and light-curve release, Astrophys. J. **938,** 113 (2022).

[33] D. Brout *et al.*, The Pantheon+ analysis: Cosmological constraints, Astrophys. J. **938,** 110 (2022).

[34] A. G. Riess *et al.*, A comprehensive measurement of the local value of the Hubble constant with 1 km/s/Mpc uncertainty from the Hubble Space Telescope and the SH0ES Team, Astrophys. J. Lett. **934,** L7 (2022).

[35] N. Metropolis, A. Rosenbluth, M. Rosenbluth, A. Teller, and E. Teller, Equation of state calculations by fast computing machines, J. Chem. Phys. **21,** 1087 (1953).

[36] W. Hastings, Monte Carlo sampling methods using Markov chains and their applications, Biometrika **57,** 97 (1970).

[37] A. Lewis, GetDist: A Python package for analysing Monte Carlo samples, arXiv:1910.13970.

[38] D. J. Spiegelhalter, N. G. Best, B. P. Carlin, and A. van der Linde, Bayesian measures of model complexity and fit, J. R. Stat. Soc. **64,** 583 (2002).

[39] A. Heavens, Y. Fantaye, E. Sellentin, H. Eggers, Z. Hosenie, S. Kroon, and A. Mootoovaloo, No evidence for extensions to the standard cosmological model, Phys. Rev. Lett. **119,** 101301 (2017).

[40] R. E. Keeley and A. Shafieloo, Ruling out new physics at low redshift as a solution to the H_0 tension, Phys. Rev. Lett. **131,** 111002 (2023).

[41] R. L. Workman *et al.* (Particle Data Group), Review of particle physics, Prog. Theor. Exp. Phys. **2022,** 083C01 (2022).